Tracking of Human Sperm in Time-Lapse Images

Chizhong Wang*, Ji-won Choi*, Leonardo F. Urbano†, Puneet Masson‡, Matthew VerMilyea §, and Moshe Kam*

*Department of Electrical and Computer Engineering, New Jersey Institute of Technology, Newark, NJ, USA
Email: {cw278, jc423, moshe.kam}@njit.edu
†70 Beharrel St., Concord, MA, USA
Email: {leonardo.f.urbano}@gmail.com
‡Penn Fertility Care, Hospital of the University of Pennsylvania, Philadelphia, PA, USA
Email: {Puneet.Masson}@uphs.upenn.edu
§Ovation Fertility, Austin, TX, USA
Email: {mvermilyea}@ovationfertility.com

Abstract—Human sperm motility analysis is a key method in assessing male fertility. It was suggested that performance of automatic sperm motility analysis systems can be enhanced by adopting multi-target tracking algorithms developed originally for radar technology. We review and appraise several target tracking algorithms operating on synthetic and actual sperm images and compare their performance. Simulations and observations of images of real sperm cells suggest that the joint probability data association filter with track-coalescence-avoiding (JPDA*) outperforms other evaluated algorithms. This is also the result obtained on images of swimming tadpoles.

Index Terms—human sperm tracking, sperm motility, performance evaluation, tracking algorithm

I. INTRODUCTION

Measures of sperm motility have been used for decades to evaluate male fertility in clinical andrology. Several techniques are being used for estimation of sperm motility [1], [2]. The most common method uses microscopes or cameras operated by technicians who count sperm cells and assess their characteristics using manual measurements. In this process, sperm motion quality is appraised visually according to standard protocols. Another class of widely used tools is computer-assisted sperm analysis (CASA) systems. CASA systems have the potential to provide fast, automatic and more objective sperm analysis than analysis relying on human operation and were the subject of several studies (i.e., [3]- [4]). These studies discussed methodologies, algorithms and results of experiments. Some authors ([5], [6]) opined that some commercial CASA machines are deficient in their ability to dispose track coalescences, which diminish their ability to perform sperm trajectory reconstruction. If wrong track reconstruction data are used in the analysis, values of key kinematic parameters may not be calculated correctly.

It was suggested ([7] - [9]) that radar tracking algorithms such as the probabilistic data association (PDA) filter and the joint probabilistic data association (JPDA) filter have potential to assist in automatic sperm analysis system. Since achieving precise ground truth tracks information from video clips of real sperm swimming is infeasible, a possible alternative is to apply candidate tracking algorithms to synthetic moving sperm images, based on mathematical models of sperm swimming.

For this study, we created video simulations of human sperm motion. We used them to compare four (4) algorithms applied to automatic sperm analysis. The mean optimal sub-pattern assignment (OSPA) distance ([10]) was used as performance criterion. Four multi-target tracking algorithms were compared; they are the nearest-neighborhood (NN), probabilistic data association (PDA), joint probabilistic data association (JPDA) and joint probabilistic data association with track-coalescence-avoiding (JPDA*). Performance of different algorithms was also compared using images of real human sperms and of swimming tadpoles video clips. Results demonstrated that the JPDA* outperforms the NN, the PDA and the JPDA algorithms in these applications.

A. Organization of the paper

Section II describes the swimming models of sperm cells. These are used to synthesize test images. In section III we use four algorithms for sperm cells tracking. These are the NN, the PDA, the JPDA and the JPDA* algorithms. In section IV we compare the algorithms and show examples of their operations (on synthetic, real sperm cells and tadpole images).

II. VIDEO SIMULATION OF SPERM MOTION

It is not feasible to compare the accuracy of different tracking algorithms using real sperm movement video clips, since ground truth on the exact sperm tracks is not available. Based on analysis of sperm swimming behavior presented by [11], we developed video simulations of swimming sperms. Using this simulation, tracking accuracy of different algorithms can be quantitatively assessed. The sperm movement video simulations contain four types of sperm motion.

1) Linear: sperm cells with this motion category move in a "ribbon" pattern path. As shown in Fig. 1 the sperm rolls side to side by following a ribbon pattern. The center of the ribbons constitute a straight-line track.

In our simulation, each sperm with linear movement has a constant path velocity drawn from a Gaussian distribution $\mathcal{N}(\mu_l, \sigma_l^2)$.

The relevant variables associated with linear movement are:

- r_h : width of ribbon

- r_v : height of ribbon
- θ_{rotation} : direction of forward movement
- V : straight line path velocity of ribbon center
- $\delta\theta_{ln}$: rate of change in ribbon angle
- x_p, y_p : x and y coordinate of simulated sperm
- x_n, y_n : x and y coordinate of ribbon center

$$\begin{bmatrix} x_p \\ y_p \end{bmatrix} = R * \begin{bmatrix} \frac{r_v}{2}\sin(2\theta_{ln}) \\ \frac{r_h}{2}\sin(\theta_{ln}) \end{bmatrix} + \begin{bmatrix} x_n \\ y_n \end{bmatrix} \quad (1)$$

where

$$R = \begin{bmatrix} \cos(\theta_{\text{rotation}}) & -\sin(\theta_{\text{rotation}}) \\ \sin(\theta_{\text{rotation}}) & \cos(\theta_{\text{rotation}}) \end{bmatrix} \quad (2)$$

$$V_x = V\cos(\theta_{\text{rotation}}) \quad (3)$$

$$V_y = V\sin(\theta_{\text{rotation}}) \quad (4)$$

$$\theta_{ln+1} = \theta_{ln} + \delta\theta_{ln} \quad (5)$$

$$x_{n+1} = x_n + V_x \quad (6)$$
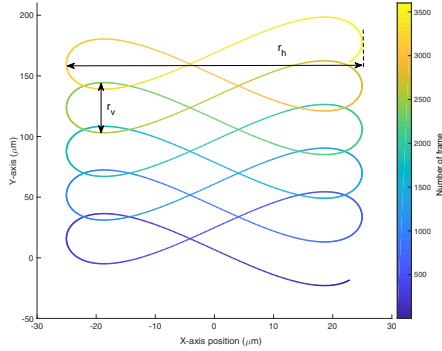
$$y_{n+1} = y_n + V_y \quad (7)$$

Fig. 1. Example realization of linear movement sperm track

2) Circular: sperm cells move in a circular pattern which is modulated by a superimposed sinusoidal movement, as shown in Fig. 2.

The relevant variables associated with circular movement are :

- r_c : radius of the circular path
- f_c : frequency of sinusoid on the circular path
- a : amplitude of the sinusoid
- $\delta\theta_{cn}$: rate of change in angle

$$x_p = [r_c + a\sin(f_c\theta_{cn})]\cos(\theta_{cn}) \quad (8)$$

$$y_p = [r_c + a\sin(f_c\theta_{cn})]\sin(\theta_{cn}) \quad (9)$$

$$\theta_{cn+1} = \theta_{cn} + \delta\theta_{cn} \quad (10)$$

3) Hyper-active: sperm cells in this category have rapid random movement in random directions. In our simulation, they are simulated following Brownian motion. The example of hyper-active track is shown in Fig. 3.

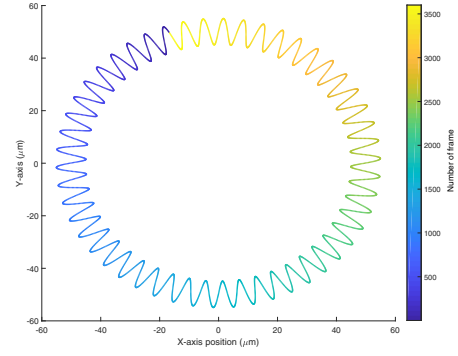The relevant variables associated with hyper-active movement are :

Fig. 2. Example realization of circular movement sperm track

- d_{rx}, d_{ry} : random displacement along x and y axes follow a normal distribution $\mathcal{N}(\mu_h, \sigma_h^2)$.

$$x_{p+1} = x_p + d_{rx} \quad (11)$$
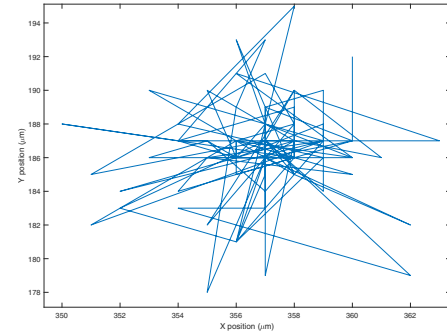
$$y_{p+1} = y_p + d_{ry} \quad (12)$$

Fig. 3. Example realization of hyper-active movement sperm track

4) Dead: dead cells are sperm cells with little or no movement. These cells are simulated as a scaled Brownian motion with relatively small speed in our setup. They are moved primarily by the fluid in which they are immersed.

The relevant variables associated with dead pattern are :

- d_{dx}, d_{dy} : random displacement along x and y axes follow a normal distribution $\mathcal{N}(\mu_h, \sigma_h^2)$.
- s : Scale coefficient.

$$x_{p+1} = x_p + sd_{dx} \quad (13)$$

$$y_{p+1} = y_p + sd_{dy} \quad (14)$$

III. TRACKING ALGORITHMS

A. Dynamic Model for Sperm Tracking

To track sperm cells we use multiple-target tracking algorithms that process a series of continuous time-lapse images. They generate tracks which consist of sequence of target state estimates. The state vector $\mathbf{x}_m$ of the m-th sperm cell is defined as

$$\mathbf{x}_m(n) = [x_m(n), y_m(n), \dot{x}_m(n), \dot{y}_m(n)]^T \quad (15)$$

198

TABLE I
COMPARISON OF TRACKING ALGORITHMS

Algorithm	Relative Performance	Computational Complexity	Ability of Avoiding Track Coalescence
NN	Poor	Low	Low
PDA	Poor	Low	Low
JPDA	Fair	Medium	Medium
JPDA*	Good	High	High

where $x_m(n)$, $y_m(n)$ are the 2D target location and $\dot{x}_m(n)$ and $\dot{y}_m(n)$ are velocity at frame (time) n. The state model is assumed as

$$\mathbf{x}_m(n+1) = \mathbf{F}\mathbf{x}_m(n) + \mathbf{w}_m(n) \qquad (16)$$

where the state transition matrix $\mathbf{F}$ is

$$\mathbf{F} = \begin{bmatrix} 1 & 0 & T & 0 \\ 0 & 1 & 0 & T \\ 0 & 0 & 1 & 0 \\ 0 & 0 & 0 & 1 \end{bmatrix}. \qquad (17)$$

Here, T is the sampling period and $\mathbf{w}_m(n)$ is the 4×1 zero mean random process noise vector with covariance matrix

$$\mathbf{Q} = q \begin{bmatrix} \frac{T^3}{3} & 0 & \frac{T^2}{2} & 0 \\ 0 & \frac{T^3}{3} & 0 & \frac{T^2}{2} \\ \frac{T^2}{2} & 0 & T & 0 \\ 0 & \frac{T^2}{2} & 0 & T \end{bmatrix}, \qquad (18)$$

where q represents the power spectral density of process noise, which indicates the process noise intensity.

A measurement $\mathbf{z}_m$ (target position plus noise) is given by

$$\mathbf{z}_m(n) = \mathbf{H}\mathbf{x}_m(n) + \mathbf{e}_m(n) \qquad (19)$$

where the measurement matrix is

$$\mathbf{H} = \begin{bmatrix} 1 & 0 & 0 & 0 \\ 0 & 1 & 0 & 0 \end{bmatrix}. \qquad (20)$$

The $\mathbf{e}_m(n)$ represents the 2×1 zero mean stationary white position noise vector with covariance matrix $\mathbf{N}$ which is given by

$$\mathbf{N} = \begin{bmatrix} \sigma_e^2 & 0 \\ 0 & \sigma_e^2 \end{bmatrix}. \qquad (21)$$

B. Operations of the tracking algorithms

The purpose of a tracking algorithm is to produce a reliable estimate $\hat{x}_m(n)$ which would be close to the true position $x_m(n)$ in some sense, for each target. Most current multiple-target tracking algorithms were introduced originally for radar applications. Beresford-Smith and Van Helden first applied radar tracking algorithms to sperm tracking by adapting the probabilistic data association (PDA) filter to track a single sperm in clutter [7]. Other multiple-target tracking algorithms were proposed for sperm tracking in [8]. Sperm tracking systems use multiple-target tracking algorithms for analyzing a series of continuous time-lapse images, to generate a tagged temporal sequence of state estimations, i.e., a track,

for each sperm. We compare four (4) algorithms used for this task: the nearest-neighborhood (NN), the probabilistic data association (PDA) algorithm, the joint probabilistic data association (JPDA) and the joint probabilistic data association with track-coalescence-avoiding (JPDA*). A brief summary and comparison of these algorithms is shown in Table I which is based on [16, p.56]. In Table I the JPDA* is described as having better relative performance and higher computational complexity than the JPDA, PDA, and NN algorithms.

The nearest neighbor tracking algorithm updates each track assuming that the nearest measurement to a track is correct [12]. It is a simple algorithm which is easy to implement. However, it is not ideal for sperm tracking systems since it assumes perfect measurement association (one observation will only be used for each track). This assumption makes the NN algorithm incapable of dealing with track coalescence. The PDA filter and the JPDA filter are two commonly used statistical algorithms based on Kalman filtering. Often they exhibit better performance than the NN algorithm. In the PDA algorithm, the posterior association probabilities are calculated for each validated measurement at the current time, to form a weighted sum of innovations for updating the target's state. The PDA algorithm is not ideal for sperm tracking systems since it does not consider the existence of other targets in the clutter. To overcome the drawbacks of PDA, JPDA was proposed. Unlike the PDA, JPDA calculates the association probability jointly over all its validated measurements at the current time to update each track [13].

The JPDA algorithm typically exhibits good performance in radar applications which have small number of targets in the environment [13]. However, it suffers from track coalescence and bias in dense target scenarios [14]. To address some of these challenges an enhanced version of JPDA, JPDA*, was introduced in [15]. The superscript "*" represents "track-coalescence-avoiding." The key difference between JPDA and JPDA* is that instead of calculating exhaustively all feasible joint association events as is done by JPDA, only the best joint association event is used in computation for each set of detected targets and set of measurements. As a result, JPDA* tends to outperform JPDA in dense target scenarios [15].

Based on the literatures it appears that in the environments that contain small number of targets, the NN, PDA, JPDA and JPDA* algorithms should have similar performance. The JPDA* is expected to outperform the others in dense target scenarios.

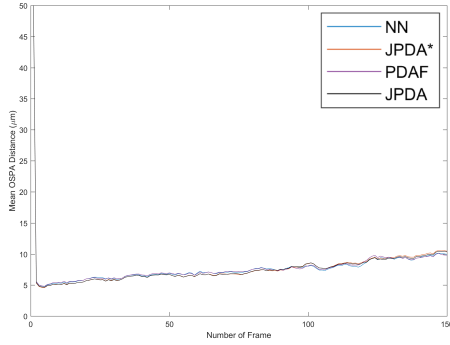Additional details on these tracking algorithms are available

Fig. 4. Comparison of four data algorithm using synthetic videos with 10 sperm cells in a 710 by 710 pixels window
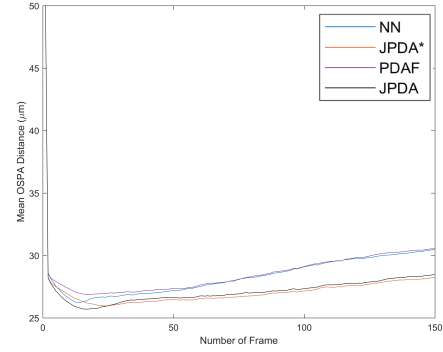

Fig. 5. Comparison of four data algorithm using synthetic videos with 200 sperm cells in a 710 by 710 pixels window

in [16].

IV. TRACKING SPERMS IN SYNTHETIC AND REAL IMAGES

A. Comparison of Data Association Algorithm Performance with Synthetic Video Clips

Fig. 4 and Fig. 5 show tracking performance of the four algorithms in two scenarios. Both scenarios share the same image size (710×710) and frame rate (15 frames per second). Fig. 4 shows the result of processing images containing 10 moving sperm cells. Fig. 5 shows the result of processing images containing 200 cells. Each set of video clips contain 10 percent of dead, 10 percent of hyper-active, 30 percent of circular and 50 percent of linear motion sperm cells. To evaluate the performance of each algorithm over frame (time), the mean optimal subpattern assignment (OSPA) distance metric between estimated and true tracks were calculated by averaging the OSPA distance over 100 replications. The OSPA measurement was suggested in [10] as a consistent assessment of tracking algorithms performance. A smaller OSPA represents better tracking performance.

All algorithms have similar performance under the sparse particle scenario as shown in Fig. 4. However, by comparing Fig. 4 to Fig. 5, we note that with larger number of sperm cells in the synthetic video clips, the performance difference among four tracking algorithms becomes more obvious and all algorithms tend to have larger OSPA distance (more sperm cells are introduced which will lead to more cell collisions). Moreover, as time elapses, all algorithms tend to have larger mean OSPA distance due to a growing number of cell collisions introduced by the movement of sperm cells.

The JPDA and JPDA* algorithms consistently exhibit better performance than the NN and PDA algorithms in both simulated scenarios. JPDA* outperforms all other algorithms in dense sperm cells scenarios since it is capable of reducing tracking coalescence.

The JPDA* and NN algorithms were also applied to video recorded from real human semen sample and from tadpole swimming videos. Human semen samples used in our study were collected and processed by the In-Vitro Fertilization
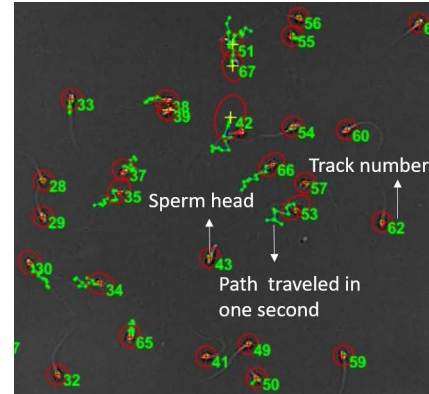

Fig. 6. Full screen snapshot of tracking generated by JPDA*

laboratories which located at Penn Fertility Care in accordance with policies of the University of Pennsylvania [9]. The videos of semen samples were recorded with resolution of 640 × 480 at 15 fps and 200×magnification (0.857 μm/pixel). A full screen representative tracking result generated by JPDA* is shown in Fig. 6. 100 μm^2 representative snapshots are shown in Fig. 7 and Fig. 8. In these figures, red cross indicates the location of sperm head and the green line represents the path that one cell traveled within 1 second. The track number is shown by the number close to the sperm.

B. Representatie Examples of Real Video Tracking Analysis

Snapshots in Fig. 7 (a) - (d) show the tracks generated by NN. The results with JPDA* applied to the same data are shown in Fig. 7 (e) - (h). As shown in Fig. 7 (a) and (e), the sperms with track number 35 and 37 are close to each other at the initial point. They 'met' with each other halfway and further collided as shown in Fig. 7 (b) - (c) and Fig. 7 (f) - (g). The performance difference between NN and JPDA* is revealed after the two sperms separated from each other as shown in Fig. 7 (d) and (h). The snapshot generated by NN shows that the sperm with track number 37 was changed erroneously to a new track (number 87) after the collision. Sperm with number track 35 also changed to track number 37 at the same time. This outcome demonstrates the inability

200

of the NN algorithm to handle collision. In contrast, JPDA*
identified and solved the collision situation perfectly as shown
in Fig. 7 (h) that after the collision the sperm cells maintained
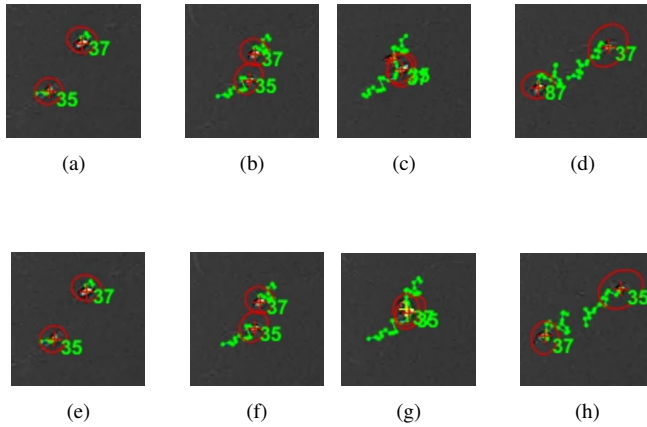the track numbers they had before the collision.

(a) (b) (c) (d)

(e) (f) (g) (h)

Fig. 7. Snapshots of multi-sperm tracking. (a) - (d) Tracking results generated
by NN. (e) - (h) Tracking results generated by JPDA*.

We also applied the NN and JPDA* algorithms to video of
swimming tadpoles which exhibit similar movement as human
sperm. The tadpole swimming video clip was obtained from
[17]. This video clip was recorded with resolution of 1280 ×
720 at 30 fps. Tracking of the swimming tadpoles shown in
Fig.8 (a) - (d) were generated with the NN algorithm. Fig.
8 (e) - (h) show the results generated from the same images
by JPDA* algorithm. The results show similar trends to these
observed in processing human sperm video clips. Tadpoles
with track number 87 and 840 were close to each other and
started to move closer as indicated in Fig. 8 (a-b) and Fig. 8
(e) - (f). Fig. 8 (c) and Fig. 8 (g) show a collision between
these tadpoles. After they separated from each other, the NN
algorithm classified them erroneously. The tadpole originally
with track number 840 changed to track number 1543. On
the other hand, JPDA* still exhibited high performance in
disposing collision situation as shown in Fig. 8 (h); after the
collision, the two tadpoles maintained the same track numbers
they had before collision.

V. CONCLUSION

We compared the performance of four (4) multi-target track-
ing algorithms, namely: nearest-neighborhood (NN), proba-
bilistic data association (PDA), joint probabilistic data associa-
tion (JPDA) and joint probabilistic data association with track-
coalescence-avoiding (JPDA*) by applying them to synthetic
human sperm images, real sperm images, and images of
swimming tadpoles. The JPDA* algorithm met or exceeded
the performance of the NN, the PDA and the JPDA algorithms
in all studied scenarios.

REFERENCES

[1] D. Mortimer, "Objective analysis of sperm motility and kinematics,".
Handbook of the Laboratory Diagnosis and Treatment of Infertility, Boca
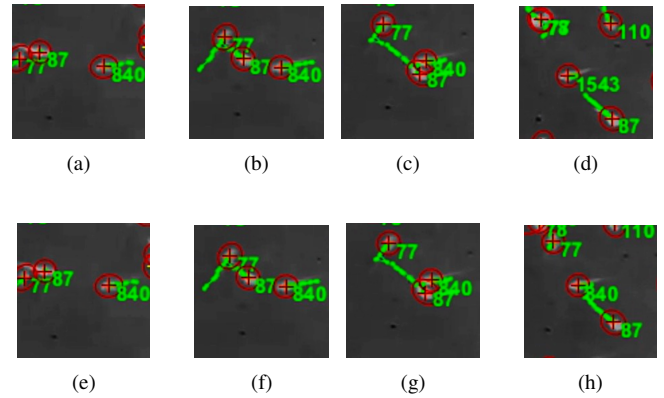Raton: CRC Press, Inc, pp. 97-133, 1990.

(a) (b) (c) (d)

(e) (f) (g) (h)

Fig. 8. Snapshots of multi-tadpoles tracking. (a) - (d) Tracking results
generated by NN. (e) - (h) Tracking results generated by JPDA*.

[2] R.P. Amann and D.F. Katz, 2004. "Andrology lab corner: Reflections on
CASA after 25 years," *Journal of Andrology*, vol. 25, no. 3, pp. 317-325,
May. 2004.
[3] M. J. Zinaman, M. L. Uhler, E. Vertuno, S.G. Fisher and E.D. Clegg,
"Evaluation of computer–assisted semen analysis (CASA) with IDENT
stain to determine sperm concentration," *Journal of Andrology*, vol 17,
no. 3, pp. 288-292, May. 1996.
[4] S. T. Mortimer, "A critical review of the physiological importance
and analysis of sperm movement in mammals," *Human Reproduction
Update*, vol. 3, no. 5, pp. 403-439, Sep. 1997.
[5] S. T. Mortimer and M. A. Swan, "Variable kinematics of capacitating
human spermatozoa," *Human Reproduction*, vol. 10, no. 12, pp. 3178-
3182, Dec. 1995.
[6] B. C. Gladen, J. Williams and R. E. Chapin, "Issues in the statistical
analysis of sperm motion data derived from computer-assisted systems,"
Journal of andrology, vol. 12, no. 2, pp. 89-96, Mar. 1991.
[7] B. Beresford-Smith and D. F. Van Helden, "Applications of radar track-
ing algorithms to motion analysis in biomedical images," *Proceedings
of 1st International Conference on Image Processing*, Austin, TX, vol. 1,
pp. 411-415, 1994.
[8] L. Sørensen, J. Østergaard, P. Johansen and M. de Bruijne, "Multi-object
tracking of human spermatozoa." *Medical Imaging*, International Society
for Optics and Photonics, 2008.
[9] L. F. Urbano, P. Masson, M. VerMilyea and M. Kam, "Automatic Track-
ing and Motility Analysis of Human Sperm in Time-Lapse Images,"
IEEE Transactions on Medical Imaging, vol. 36, no. 3, pp. 792-801,
Mar. 2017.
[10] B. Ristic, B. N. Vo, D. Clark and B. T. Vo, "A metric for performance
evaluation of multi-target tracking algorithms," *IEEE Transactions on
Signal Processing*, vol.59, no.7, pp.3452-3457, Jul. 2011.
[11] D. F. Babcock, G. Wennemuth and P.M. Wandernoth, "Episodic rolling
and transient attachments create diversity in sperm swimming behavior".
BMC biology, vol. 12, no. 1, p.67, Dec. 2014.
[12] S. Blackman and R. Popoli, *Design and Analysis of Modern Tracking
Systems*, Norwood, MA, USA: Artech House, 1999.
[13] D. F. Crouse, Y. Bar-Shalom, P. Willett and L. Svensson, "The JPDAF
in practical systems: Computation and snake oil," *Proceedings of SPIE:
Signal and Data Processing of Small Targets Conference*, vol. 7698, Apr.
2010.
[14] P. Jing, S. Xu, X. Li and Z. Chen, "Coalescence-avoiding joint proba-
bilistic data association based on bias removal," *EURASIP Journal on
Advances in Signal Processing*, vol. 24, no.1, Dec. 2015.
[15] E. A. Bloem and H. A. P. Blom, "Joint probabilistic data association
methods avoiding track coalescence," *Proceedings of 1995 34th IEEE
Conference on Decision and Control*, vol. 3, pp. 2752-2757, 1995.
[16] Y. Bar-Shalom, *Multitarget-multisensor tracking: advanced applications*,
Artech House, 1990.
[17] MacbthPSW, "Tadpoles swimming," [online] Available at:
www.youtube.com/watch?v=K3ySu5M3vs [Dec. 10, 2017].